

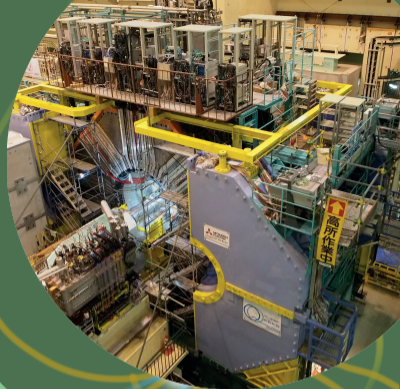
OVERVIEW OF τ LEPTON FLAVOUR VIOLATING DECAYS AT BELLE II

GDR-InF Annual Workshop 2022

Friday 4th November, 2022

Robin Leboucher
Léonard Polat

Aix Marseille Univ, CNRS/IN2P3, CPPM, Marseille, France



Outline



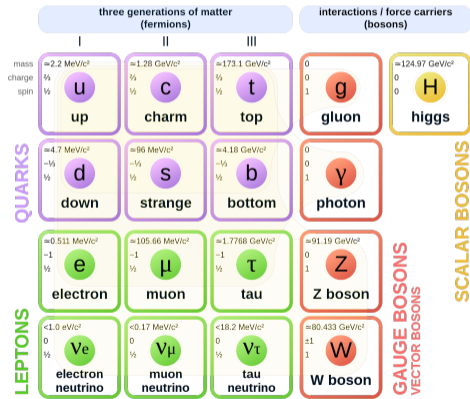
- Lepton flavour violation (LFV) in τ decays
- Overview of the Belle II experiment
- Search for $\tau \rightarrow \ell \phi$ (L. Polat)
- Search for $\tau \rightarrow \mu \mu \mu$ (R. Leboucher)
- Other τ LFV channels at Belle II

The τ lepton

τ ID Card

- Discovery: 1974-1977 at SLAC-LBL, California
- Mass: $1.777 \text{ GeV}/c^2$ (heaviest lepton)
- Lifetime: $\sim 290.3 \times 10^{-15} \text{ s}$ ($10^7 \times$ shorter than muons)
- Main τ^- decays (95%):
 - $e^- \bar{\nu}_e \nu_\tau$ or $\mu^- \bar{\nu}_\mu \nu_\tau$
 - $\pi^- \nu_\tau$
 - $\pi^- \pi^0 (\pi^0) \nu_\tau$
 - $\pi^- \pi^+ \pi^- (\pi^0) \nu_\tau$

Standard Model of Elementary Particles



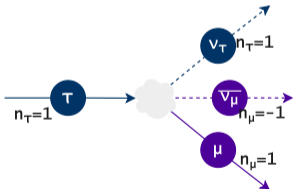


The Lepton Flavour Violation in the Standard Model

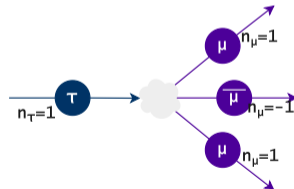
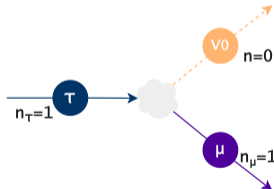
Lepton Flavour Violation

→ when lepton flavour numbers are not conserved between the initial and final states of a decay.

Lepton Flavour conservation



Lepton Flavour violation



Flavour-Changing Neutral Currents

Neutrino oscillations

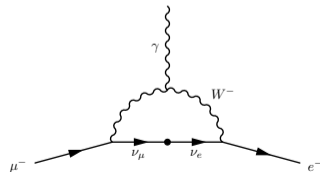
- The only source of lepton flavour violation in the Standard Model.
- First evidence in 1998 by Super-Kamiokande.
- Implies that neutrinos have masses.
- Described by the Pontecorvo–Maki–Nakagawa–Sakata matrix.

$$\underbrace{\begin{pmatrix} \nu_e \\ \nu_\mu \\ \nu_\tau \end{pmatrix}}_{\text{Flavour eigenstates}} = \underbrace{\begin{pmatrix} U_{e1} & U_{e2} & U_{e3} \\ U_{\mu 1} & U_{\mu 2} & U_{\mu 3} \\ U_{\tau 1} & U_{\tau 2} & U_{\tau 3} \end{pmatrix}}_{\text{PMNS matrix}} \underbrace{\begin{pmatrix} \nu_1 \\ \nu_2 \\ \nu_3 \end{pmatrix}}_{\text{Mass eigenstates}}$$

FCNC in the SM

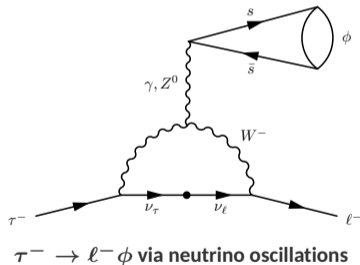
- Neutrino oscillations introduce FCNC via W^\pm boson loops.
- Processes heavily suppressed, with rates **below** $\mathcal{O}(10^{-50})$.

Example: LFV decay $\mu^- \rightarrow e^- \gamma$ via neutrino oscillations:

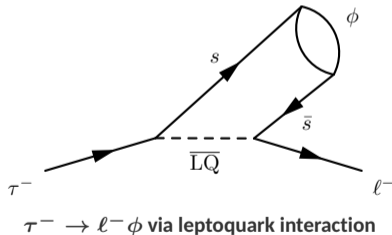


LFV in New physics - $\tau \rightarrow \ell V^0$

$\tau \rightarrow \ell V^0$ ($\ell = e, \mu$; V^0 : neutral vector meson) LFV decays can be enhanced in many new physics models: MSSM, Type-III Seesaw, $SO(10)$ GUT, SM + Heavy Dirac Neutrinos, Littlest Higgs Model with T-parity, Unparticles...

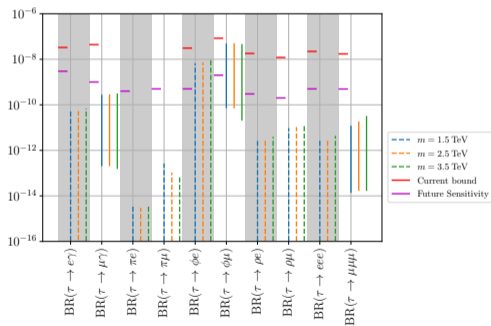


$\tau \rightarrow \ell \phi$ ($\phi = s\bar{s}$ meson of mass $\sim 1020 \text{ MeV}/c^2$) in particular is related to the U_1 vector leptoquark hypothesis \rightarrow could explain both $R_{D^{(*)}}$ and $R_{K^{(*)}}$ anomalies.



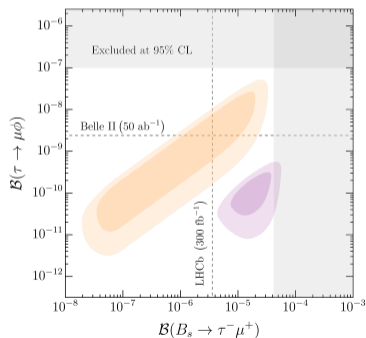
LFV in New physics - $\tau \rightarrow \ell V^0$

$\tau \rightarrow \ell V^0$ ($\ell = e, \mu$; V^0 : neutral vector meson) LFV decays can be enhanced in many new physics models: MSSM, Type-III Seesaw, $SO(10)$ GUT, SM + Heavy Dirac Neutrinos, Littlest Higgs Model with T-parity, Unparticles...



C. Hati et al., Eur.Phys.J.C 81 (2021) 12, 1066

$\tau \rightarrow \ell \phi$ ($\phi = s\bar{s}$ meson of mass ~ 1020 MeV/ c^2) in particular is related to the U_1 vector leptoquark hypothesis \rightarrow could explain both $R_{D^{(*)}}$ and $R_{K^{(*)}}$ anomalies.



C. Cornella et al., JHEP 08 (2021) 050



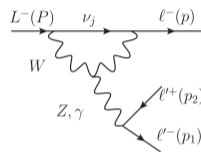
LFV in New physics - $\tau \rightarrow \ell \ell \ell$

$\tau \rightarrow \ell \ell \ell$ ($\ell = e, \mu$) LFV decays involve in:

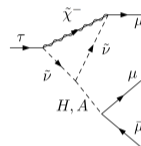
| New Physics models | Limit BF for $\tau^- \rightarrow \mu^- \mu^+ \mu^-$ |
|------------------------------|---|
| Littlest Higgs with T-parity | 10^{-8} |
| R-parity violating SUSY | 10^{-8} |
| Non-universal Z' | 10^{-8} |
| MSSM + seesaw* | 10^{-9} |
| SUSY SO(10) | 10^{-10} |
| SUSY Higgs | 10^{-10} |
| SM + heavy Majorana ν | 10^{-10} |

Giffels et al. 2008

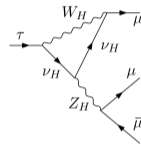
Strength: background free \Leftarrow purely leptonic final state.



(a) Neutrino oscillations



(b) see-saw MSSM



(c) Littlest Higgs with T-parity

τ LFV searches at colliders

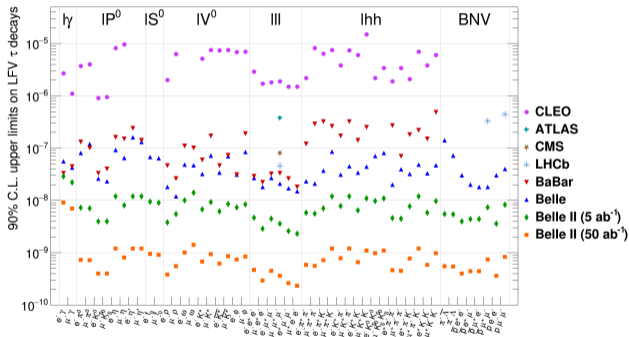
Current status

Around 50 τ LFV channels studied in the past two decades; best upper limits on branching fractions set by the Belle experiment ($10^{-8} - 10^{-7}$ range).

| Decay channel | $\mathcal{B}_{UL} \times 10^{-8}$ @90% CL | | | |
|------------------------------|---|-------|------|-----|
| | BaBar | Belle | LHCb | CMS |
| $\tau \rightarrow e\phi$ | 3.1 | 3.1 | - | - |
| $\tau \rightarrow \mu\phi$ | 19 | 8.4 | - | - |
| $\tau \rightarrow \mu\mu\mu$ | 3.3 | 2.1 | 4.6 | 8.0 |

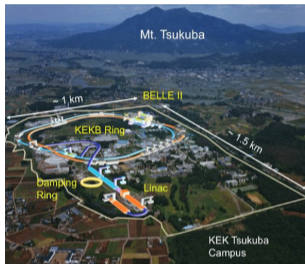
Prospects

Belle II expected to improve current limits by at least 1 order of magnitude \rightarrow sensitive to some NP models.



Banerjee et al. 2022; Kou et al. 2019

The Belle II experiment

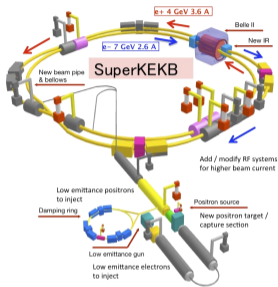


- Around 26 countries
- More than 1000 physicists
- 400 students

- Located at **KEK, Tsukuba** \rightarrow ~ 60 km from Tokyo Japan
- Upgrade of Belle and KEKB, ran from 1999 to 2010
- **SuperKEKB e^+e^- collider** of 3 km circumference
- **Data taking start in 2019**, with almost complete detector
- **1st Long shutdown** since summer 2022 to fully install PXD



SuperKEKB and status of Belle II

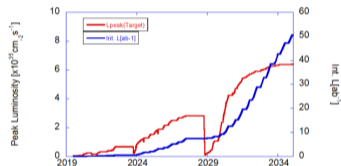
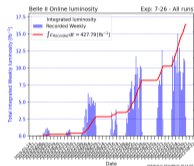


SuperKEKB

- Asymmetric Electron (7 GeV) Positron (4 GeV) collider
- Produce:
 - $e^+e^- \rightarrow \Upsilon(4S)[10.58 \text{ GeV}] \rightarrow B\bar{B}$ [$\sigma = 1.1 \text{ nb}$]
 - $e^+e^- \rightarrow \tau^+\tau^-$ [$\sigma = 0.9 \text{ nb}$]
 - and also $u\bar{u}$, $d\bar{d}$, $s\bar{s}$, $c\bar{c}$, e^+e^- , $\mu^+\mu^-$...

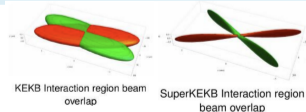
Targets

- Peak luminosity: today $4.7 \times 10^{34} \text{ cm}^{-2}\text{s}^{-1} \rightarrow$ target $\sim 6 \times 10^{35} \text{ cm}^{-2}\text{s}^{-1}$
- data collected: today $427.79 \text{ fb}^{-1} \rightarrow$ target 50 ab^{-1}

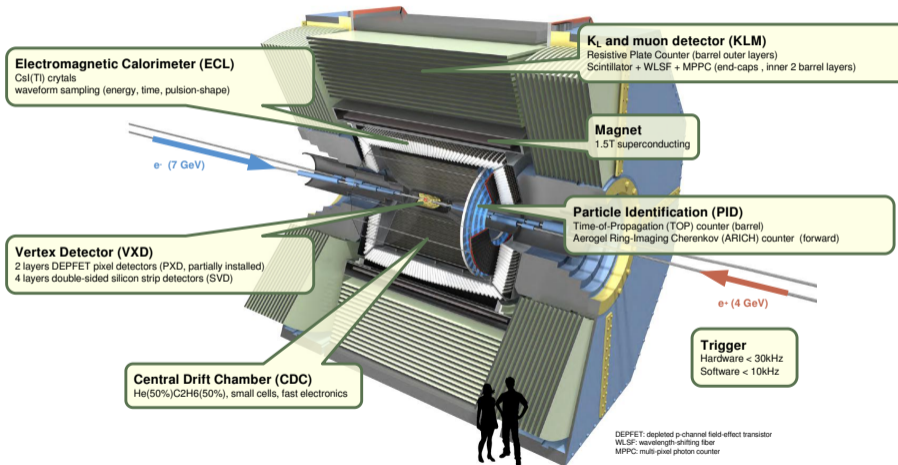


Future improvements

Higher beam currents + Lower beam size $\rightarrow 30 \times$ KEKB peak luminosity



Belle II Detector



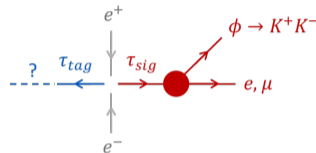
$\tau \rightarrow \ell \phi$ - Analysis strategy

“Inclusive” reconstruction

Final state of signal τ : 1 charged lepton + 2 charged kaons from ϕ resonance ($\mathcal{B} \sim 50\%$).
Oppositely charged τ (*tag*) not constrained to 1-prong decays \Rightarrow increases signal efficiency by 30%, adding:

- decays of τ_{tag} into 3-prong ($\mathcal{B} \sim 15\%$),
- events with missing track(s),
- events with additional track(s) (fake/clone/beam-induced)...

... but also other sources of background!

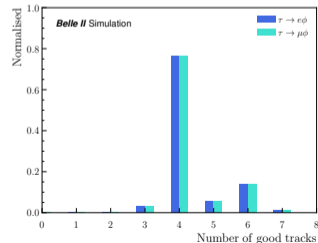


Framework

- 2D space ($M_\tau, \Delta E_\tau$) where $\Delta E_\tau = E_\tau^{\text{CM}} - \sqrt{s}/2$.
- Define a *signal region* (SR) around expected signal peak ($M_\tau \simeq 1.777, \Delta E_\tau \simeq 0$).
- SR blinded in data. Upper limit to be computed in this region.

Background suppression strategy

- Roughly defined **cut-based selection** against background with clear differences from signal in variables distributions.
- **Boosted decision trees** (BDTs) against remaining contributions.



$\tau \rightarrow \ell \phi$ - Event reconstruction

Samples

Monte Carlo simulation:

- Signal: $\tau^\pm \rightarrow e^\pm \phi$; $\tau^\pm \rightarrow \mu^\pm \phi$
- Background: $\tau^+ \tau^-$, $q\bar{q}$, $B\bar{B}$, $\ell\ell(XX)$ ($\ell = e, \mu$; $X = e, \mu, \tau, \pi, K, p$).

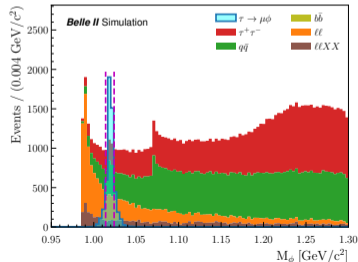
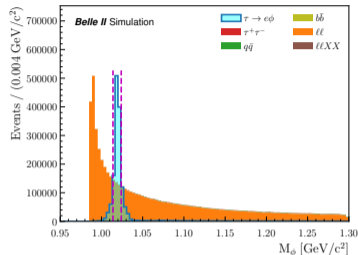
Belle II data: 189.9 fb^{-1} (2019-2021).

Event requirements

Track selections:

- Originate from the interaction point (IP): "good tracks"; at most 6 in event.
- Lepton tracks selected with particle identification variables (PID).
- Kaon tracks required to be in CDC acceptance \rightarrow no PID requirement but selection on ϕ mass instead: $1.014 < M_\phi < 1.024 \text{ GeV}/c^2$.

Events required to fire **low-multiplicity Level1 (L1) ECL triggers**.

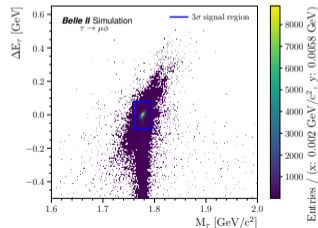
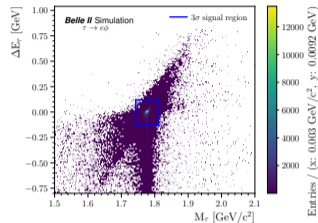


$\tau \rightarrow \ell\phi$ - Signal regions

Resolution σ computed from fit to M_τ and ΔE_τ (more details in slide 26).

- Signal region to compute the observed limit: 3σ .
- Region blinded in data: 5σ (as a precaution).
- All events constrained to: 20σ .

| | $\tau \rightarrow e\phi$ | | $\tau \rightarrow \mu\phi$ | |
|-------------------|-----------------------------------|--------------------------|-----------------------------------|--------------------------|
| | M_τ [MeV/c ²] | ΔE_τ [MeV] | M_τ [MeV/c ²] | ΔE_τ [MeV] |
| 3σ region | [1.743, 1.811] | [-0.125, 0.120] | [1.760, 1.794] | [-0.083, 0.080] |
| 5σ region | [1.721, 1.834] | [-0.207, 0.202] | [1.749, 1.805] | [-0.137, 0.134] |
| 20σ region | [1.551, 2.004] | [-0.8, 0.8] | [1.665, 1.890] | [-0.5, 0.5] |
| Resolution | 11.3 ± 0.2 | 41.0 ± 0.8 | 5.6 ± 0.2 | 27.1 ± 0.6 |



$\tau \rightarrow \ell \phi$ - Background suppression: Preselection

Signal efficiency ($\varepsilon_{\ell\phi}$) and background rejection (r_{bkg}) after other preselection criteria are applied:

| Mode | Preselection | $\varepsilon_{\ell\phi}$ (%) | r_{bkg} (%) |
|-----------|---|---------------------------------|-------------------------|
| $e\phi$ | $\theta_{\tau-\text{closest}} > 0.02$ rad | 98.9 | 53.5 |
| | CLEO thrust $0 < 8.5$ GeV/c | 97.7 | 63.1 |
| | $\theta_{K_1-K_2} > 0.01$ rad | 99.8 | 5.5 |
| | electronID of lepton > 0.9 | 91.0 | 59.7 |
| | KaonID of leading kaon > 0.6 | 67.8 | 92.2 |
| | Total (full preselection) | 58.7 | 99.7 |
| $\mu\phi$ | Thrust axis magnitude < 0.99 | 97.8 | 9.6 |
| | muonID of lepton > 0.99 | 95.2 | 27.1 |
| | KaonID of leading kaon > 0.6 | 69.3 | 80.8 |
| | Total (full preselection) | 64.5 | 89.8 |

→ $e\phi$ preselection mostly against Bhabha scattering background.

→ kaonID not very efficient, affects signal efficiency.

Punzi figure of merit

Indicator of selection performance:

$$\frac{\varepsilon_{\ell\phi}}{a/2 + \sqrt{B}}$$

$\varepsilon_{\ell\phi}$: signal efficiency; B : background yield; $a = 3$ (significance).

| | $\tau \rightarrow e\phi$ | $\tau \rightarrow \mu\phi$ |
|--|---|---|
| Signal efficiency | 10.9% (20σ) 8.5% (3σ) | 10.3% (20σ) 8.4% (3σ) |
| Background yields at 189.9 fb^{-1} | ~ 1300 (20σ) ~ 20 (3σ) | ~ 260 (20σ) ~ 4 (3σ) |
| Punzi FOM (3σ) | 0.014 | 0.024 |

→ $q\bar{q}$ continuum main background source (KKK, $\pi\pi\pi$, ...) + Bhabha for $\tau \rightarrow e\phi$.

$\tau \rightarrow \ell\phi$ - Background suppression: BDT optimisation

BDT strategy

MC simulation split into 3 samples:

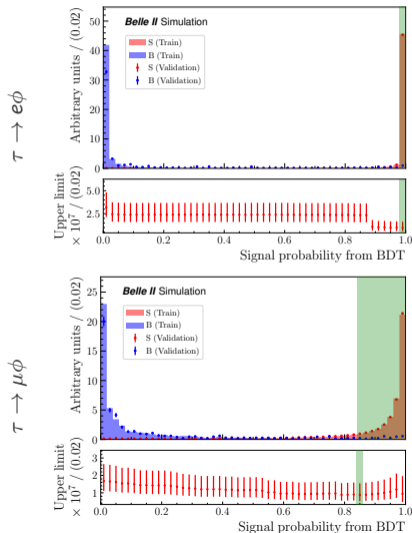
- one for the *training* of the BDT,
- one to *validate* the BDT performance,
- one to extract the expected $\varepsilon_{\ell\phi}$ and B for the limit computation.

Training carried out using the XGBoost library.

Evaluation metric: logarithmic loss function.

Optimisation of BDT selection

- Expected upper limit (90% C.L.) in validation sample as a function of the signal probability.
- CLs method, asymptotic formula (see slide 24).
- Selection at probability with smallest limit.

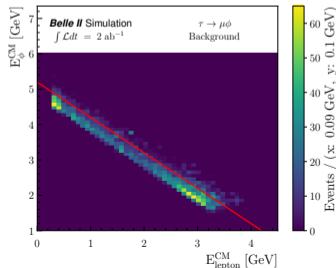
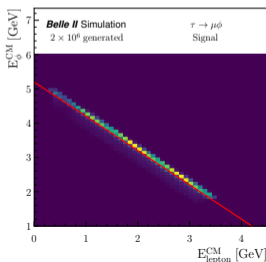
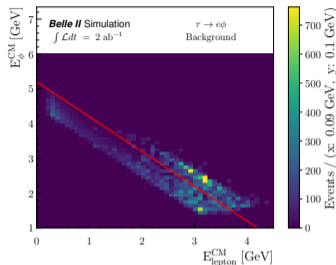
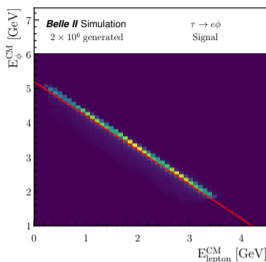


$\tau \rightarrow \ell \phi$ - Background suppression: 2- vs 3-body decays

Further background suppression against 3-body decay background:

$$E_{\phi}^{\text{CM}} > -1 \times E_{\text{lepton}}^{\text{CM}} + 5.2.$$

- $\sim 80\%$ relative signal efficiency and $\sim 85\%$ background rejection if applied before BDT training.
- Applied after BDT training to increase the statistics.



$\tau \rightarrow \ell\phi$ - Background suppression: Results

In the SR, after the full selection:

| | $\tau \rightarrow e\phi$ | $\tau \rightarrow \mu\phi$ |
|---|--------------------------|----------------------------|
| Signal efficiency | 7.9% | 7.2% |
| Background yields at 189.9 fb^{-1} | 0.92 | 0.83 |
| Punzi FOM | 0.032 | 0.030 |

Remaining backgrounds:

■ $e\phi$: $KKK, K\pi\pi, e\pi\pi, ee\pi$.

■ $\mu\phi$: $KKK, KK\pi, K\pi\pi, \pi\pi\pi, \mu\pi\pi$.

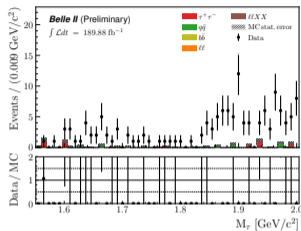
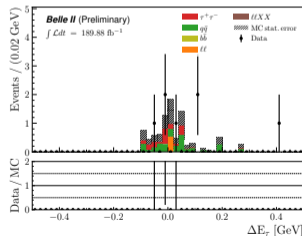
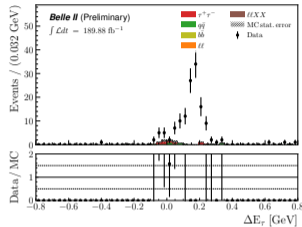
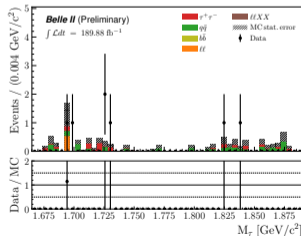
} Misidentification, underperforming kaonID.

$\tau \rightarrow \ell \phi$ - Data-MC comparison (1)

Comparison inside the *sidebands*: $5 - 20\sigma$ region in $(M_{\tau}, \Delta E_{\tau})$ space.

| | $\tau \rightarrow e \phi$ | $\tau \rightarrow \mu \phi$ |
|---------------|---------------------------|-----------------------------|
| Data yield | 138 | 7 |
| MC yield | 6.33 | 5.06 |
| Data/MC ratio | $22 \pm 4_{\text{stat}}$ | $1.4 \pm 0.6_{\text{stat}}$ |

Clear excess of data events ($\Delta E \sim 0.2$ GeV)
 \rightarrow background not simulated in MC samples.

 $\tau \rightarrow e \phi$

 $\tau \rightarrow \mu \phi$


$\tau \rightarrow \ell \phi$ - Reduction of data excess (e channel)

Nature of the data excess

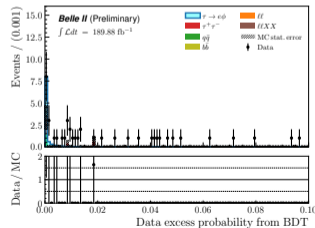
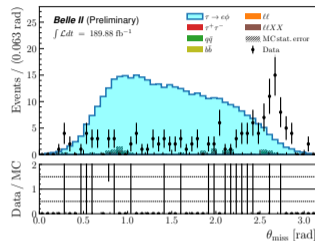
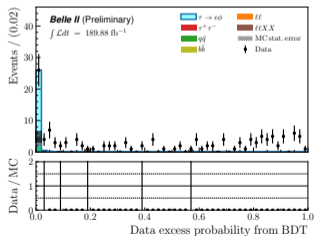
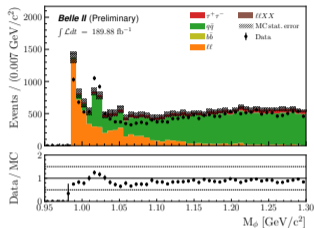
- Peak appears in data at ϕ meson mass after the preselection.
- Missing momentum in backward region (large polar angle).
- Mostly events with 4 tracks.

⇒ probably diphoton events going into hadrons with ϕ resonance, not simulated.

Data excess veto

Second BDT trained on 10% of data, before the selection, *inside the sidebands* (no unblinding).

- Target: data events in $-0.1 < \Delta E < 0.4$ GeV.
- Signal MC added as “background”.
- Veto on probability output at 0.001.





$\tau \rightarrow \ell \phi$ - Data-MC comparison (2)

*: from validation sample.

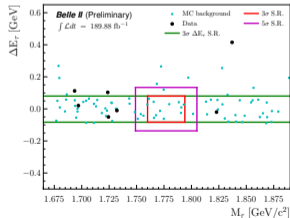
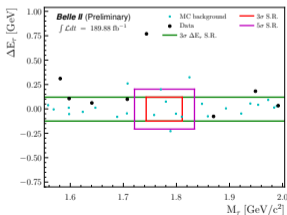
| Result | | Region | Mode | |
|--|------------------|----------|-----------------------------|-----------------------------|
| | | | $e\phi$ | $\mu\phi$ |
| Signal efficiency $\varepsilon_{\ell\phi}$ | | SR | 6.0% | 7.2% |
| MC background yield | | SB | 3.34 | 5.06 |
| | | RSB | 3.10 / 2.53* | 4.10 / 4.06* |
| Background ratio in MC | | SR | 0.38 / 0.36* | 0.83 / 0.76* |
| | | SR / RSB | 0.13 | 0.19 |
| Data yield | N_{obs} | SB | 8 | 7 |
| | N_{exp} | RSB | 5 | 4 |
| Data / MC ratio | | SR | 0.66 | 0.78 |
| | | SB | $2.4 \pm 1.0_{\text{stat}}$ | $1.4 \pm 0.6_{\text{stat}}$ |
| | | RSB | $1.6 \pm 0.8_{\text{stat}}$ | $1.0 \pm 0.5_{\text{stat}}$ |

| Result | | Experiment | Mode | |
|--|--|------------|---------|-----------|
| | | | $e\phi$ | $\mu\phi$ |
| Signal efficiency $\varepsilon_{\ell\phi}$ | | BaBar | 6.43% | 5.18% |
| | | Belle | 4.18% | 3.21% |
| Data yield N_{exp} | | BaBar | 0.68 | 2.76 |
| | | Belle | 0.47 | 0.06 |

- SR: signal region (3σ).
- SB: sidebands ($5 - 20\sigma$).
- RSB: sidebands reduced to 3σ in ΔE_{τ} .

Data yield expected in SR:

$$N_{\text{exp}} = N_{\text{obs}}^{\text{RSB}} \times \frac{N_{\text{MC}}^{\text{SR}}}{N_{\text{MC}}^{\text{RSB}}}$$



$\tau \rightarrow \ell\phi$ - Summary of uncertainties

Systematic uncertainties

- PID:** errors on PID weights, assigned to MC events as corrections according to data. *Provided by the collaboration.*
- Tracking efficiency:** equal contribution from each of the 3 signal tracks. *From tracking performance studies.*
- Trigger efficiency:** bias from low-multiplicity trigger requirements. *Measured on signal MC using orthogonal trigger lines.*
- BDT selection:** bias from data-MC discrepancies for variables in the selection. *Absolute difference with signal efficiency if corrections from control samples ($D_s \rightarrow \phi\pi$ & $\tau \rightarrow \pi\pi\nu_\tau$) are applied.*
- Momentum scale:** correction on tracking momentum bias from wrong magnetic field map used in data reconstruction process. *Provided by the collaboration.*

Systematic uncertainties

| Affected quantity | Source | Mode | |
|-----------------------|-------------------------|--------------|--------------|
| | | $e\phi$ | $\mu\phi$ |
| $\epsilon_{\ell\phi}$ | Particle identification | 0.11% | 0.16% |
| | Tracking efficiency | 0.52% | |
| | Trigger efficiency | 0.4% | 0.9% |
| | BDT selection | 0.48% | 0.95% |
| L | Luminosity | 0.6% | |
| $\sigma_{\tau\tau}$ | Tau-pair cross section | 0.003 nb | |
| N_{exp} | Momentum scale | +0.0 -0.0 | +0.0 -0.2 |

Total uncertainties

| Affected quantity | Mode | |
|---|--------------|--------------|
| | $e\phi$ | $\mu\phi$ |
| $L \times \sigma_{\tau\tau} \times \epsilon_{\ell\phi}$ | 8.25% | 13.39% |
| N_{exp} | +0.4 -0.4 | +0.4 -0.5 |

$\tau \rightarrow \ell\phi$ - Upper limit estimation

CLs method with pyhf. With n the number of expected events, s the signal and b the background:

$$E[n] = \underbrace{\mu s + b}_{\mu} = \underbrace{\mathcal{B}(\tau \rightarrow \ell\phi)}_{\mu} \times \underbrace{2L\sigma_{\tau\tau}\epsilon_{\ell\phi}}_s + b. \quad \left| \quad \text{CL}_S = \frac{\text{CL}_{s+b}}{\text{CL}_b} = 10\%.$$

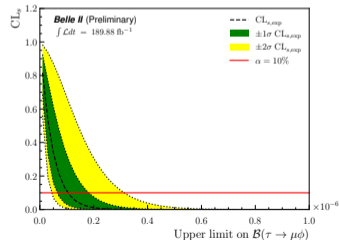
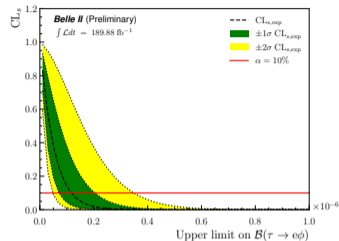
Expected upper limits at 90% C.L.:

$$\mathcal{B}_{\text{UL,exp}}^{90}(\tau \rightarrow e\phi) = 1.18 \times 10^{-7},$$

$$\mathcal{B}_{\text{UL,exp}}^{90}(\tau \rightarrow \mu\phi) = 1.05 \times 10^{-7}.$$

At equivalent luminosities (BaBar: 451 fb^{-1} ; Belle: 854 fb^{-1}):

- $\tau \rightarrow e\phi$: expected limit competitive neither with Belle nor BaBar,
- $\tau \rightarrow \mu\phi$: same expected limit as Belle, better than BaBar (-17%).



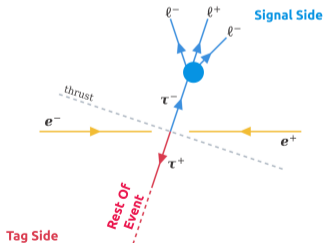
$\tau \rightarrow \mu \mu \mu$ - Inclusive reconstruction

Events reconstruction strategy

Reconstruct τ pair events with an inclusive strategy:

- Signal side: one τ decay into the LFV channel $\rightarrow \mu \mu \mu$
- Tag side: opposite one is put in a Rest of Event \rightarrow without specific decay

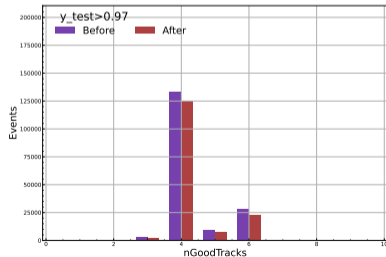
This strategy allow to cover more decays channels for the tag side and improve the reconstruction efficiency.



Reconstruction details equivalent to the $\tau \rightarrow \ell \phi$ one in **slide 14**.

Analysis strategy

- Define signal region in $M_{\mu \mu \mu}$ and $\Delta E_{\mu \mu \mu}$ plane to remove backgrounds, blind data and estimate expected background
- Reject low multiplicity backgrounds with **cut based preselection**
- Reject main contribution backgrounds with **Boosted Decision Tree**





$\tau \rightarrow \mu \mu \mu$ - Signal Region in $M_{\mu \mu \mu}$; $\Delta E_{\mu \mu \mu}$ 2D plane (1)

Measure resolutions to define a **region** around **peaking signal** at:
 $M_{\mu \mu \mu} \simeq 1.777 \text{ GeV}/c^2$ and $\Delta E_{\mu \mu \mu} = E_{\mu \mu \mu}^{\text{CM}} - \sqrt{S}/2 \simeq 0 \text{ GeV}$

Fitting mass and delta energy

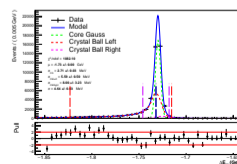
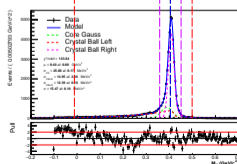
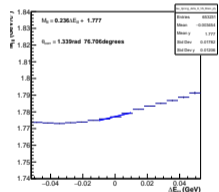
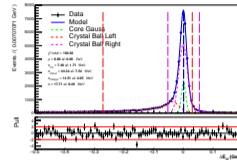
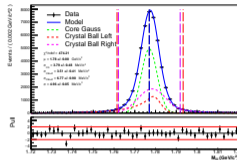
Sum 3 distributions:

- **Gaussian**: for the peak
- **2 Crystal Balls**: for both side tails

Try decorrelate variables

$$\begin{pmatrix} M'_{\mu \mu \mu} \\ \Delta E'_{\mu \mu \mu} \end{pmatrix} = \begin{pmatrix} \cos(\theta) & -\sin(\theta) \\ \sin(\theta) & \cos(\theta) \end{pmatrix} \begin{pmatrix} M_{\mu \mu \mu} \\ \Delta E_{\mu \mu \mu} \end{pmatrix}$$

with $\theta = 76.71^\circ$



| | Mean | Resolution |
|---------------------------|-------------------------------------|---------------------------------|
| $M_{\mu \mu \mu}$ | $1.7769 \pm 0.0009 \text{ GeV}/c^2$ | $4.96 \pm 0.05 \text{ MeV}/c^2$ |
| $\Delta E_{\mu \mu \mu}$ | $0.0005 \pm 0.0004 \text{ GeV}$ | $17.71 \pm 0.48 \text{ MeV}$ |
| $M'_{\mu \mu \mu}$ | 0.4044 ± 0.0008 | 15.47 ± 0.09 |
| $\Delta E'_{\mu \mu \mu}$ | -1.7319 ± 0.0003 | 4.64 ± 0.03 |

$\tau \rightarrow \mu \mu \mu$ - Signal Region in $M_{\mu\mu\mu}$; $\Delta E_{\mu\mu\mu}$ (2)

Use signal region as background suppression

We define several condition with:

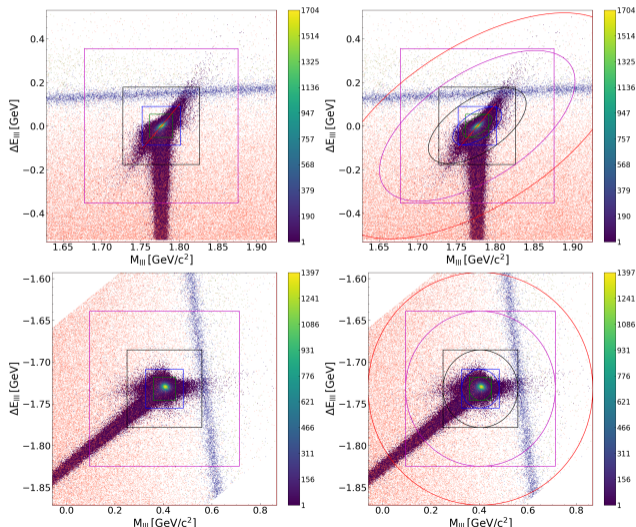
- different variable (rotated or not)
- different shape (boxes or ellipse)
- different sizes (3 or 5 resolution width)

No normalization, no weights:

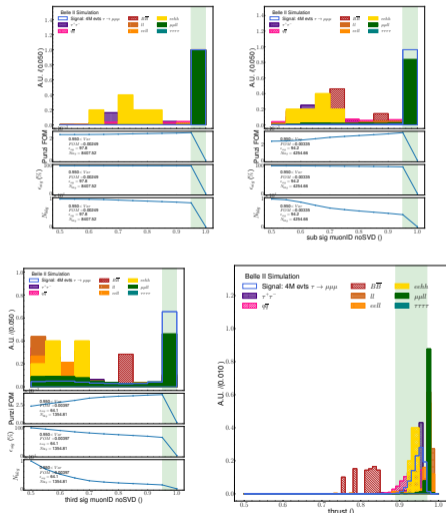
| | Var | ϵ_{sig} (%) | N_{bkg} |
|---|--------------------|----------------------|-----------|
| 3 | M ; ΔE | 22.05 | 372 |
| 3 | <i>Ellipse</i> | 21.62 | 286 |
| 3 | M' ; $\Delta E'$ | 21.82 | 295 |
| 3 | <i>Ellipse'</i> | 21.40 | 241 |

To blind

Blind data according to the signal region, only use side-bands, where we also estimate the background.



$\tau \rightarrow \mu \mu \mu$ - Background suppression: Preselections



Preselections

Define set of preselection to mainly reject background:
 $e^+e^- \rightarrow e^+e^-$ (Bhabha), $e^+e^- \rightarrow \mu^+\mu^-$, $e^+e^- \rightarrow \ell\ell X X$

Normalized for $400\ fb^{-1}$:

| | MuonID | Preselection | $\epsilon_{sig} (\%)$ | N_{bkg} |
|----------------------------|--------|------------------------------|-----------------------|-----------|
| $\mu ID^{lead} > 0.95$ | | $0.89 < thrust < 0.97$ | 22.80 | 1736.71 |
| $\mu ID^{lead} > 0.95$ | | $0.93 < thrustBm < 0.95$ | 23.05 | 2072.30 |
| $\mu ID^{lead} > 0.95$ | | $5.5 < E_{vis}^{CMS} < 10.5$ | 22.83 | 1546.57 |
| $\mu ID^{lead} > 0.95$ | | $0.5 < E_{mis}^{CMS} < 5.0$ | 21.40 | 857.23 |
| $\mu ID^{lead} > 0.95$ | | $p_{T_{mis}}^{CMS} > 0.2$ | 22.48 | 1108.33 |
| $\mu ID^{lead,sub} > 0.95$ | | $0.89 < thrust < 0.97$ | 21.98 | 735.71 |
| $\mu ID^{lead,sub} > 0.95$ | | $0.93 < thrustBm < 0.95$ | 22.25 | 1128.39 |
| $\mu ID^{lead,sub} > 0.95$ | | $5.5 < E_{vis}^{CMS} < 10.5$ | 22.01 | 630.03 |
| $\mu ID^{lead,sub} > 0.95$ | | $0.5 < E_{mis}^{CMS} < 5.0$ | 20.63 | 328.72 |
| $\mu ID^{lead,sub} > 0.95$ | | $p_{T_{mis}}^{CMS} > 0.2$ | 21.67 | 458.26 |

All combination (μID selection + other variable) are tested with a Boosted Decision Tree train to remove other background sources.

$\tau \rightarrow \mu \mu \mu$ - Background suppression: BDT (1)

Use BDT for background rejection

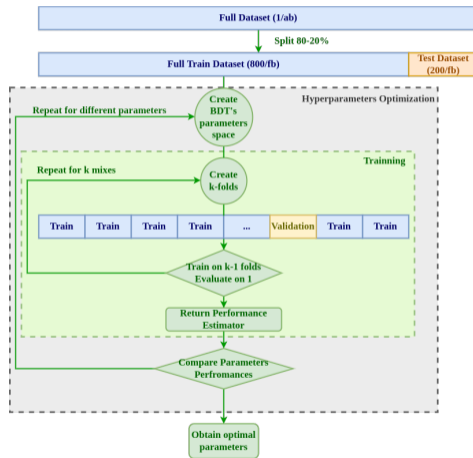
Reject backgrounds coming from continuum $q\bar{q}$ and $\tau^+\tau^-$ with a **Boosted Decision Tree (BDT)** classification
Calafiura, Rousseau, and Terao 2022.

K-Folding

Machine learning are sensible to arbitrar sample split in test/validation/test subsamples \Rightarrow **k-folds method** minimize this source of overtraining

- Split in **Train|Test**
- Split in **k-folds**:
 - Use $k - 1$ folds to train
 - Use last folds to validate
 - Repeat for all $\binom{k}{k-1} = k$ combinations
 - Average k outputs

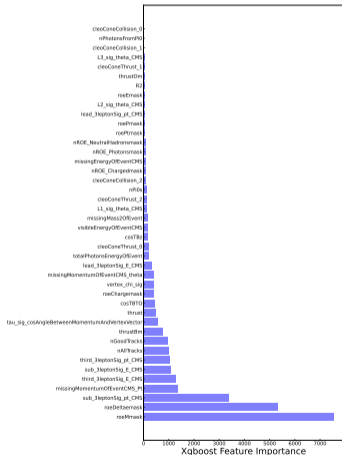
- Train BDT on Monte-Carlo Simulations
- Using python's **XGBoost** library for BDT
- Using python's **Optuna** library for optimization
- 100 Parameters setups are evaluated according to the **logarithmic loss function**





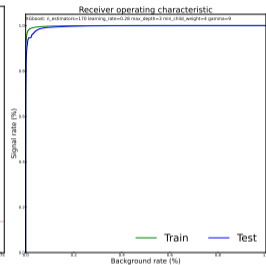
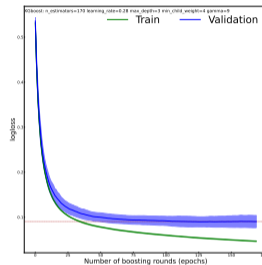
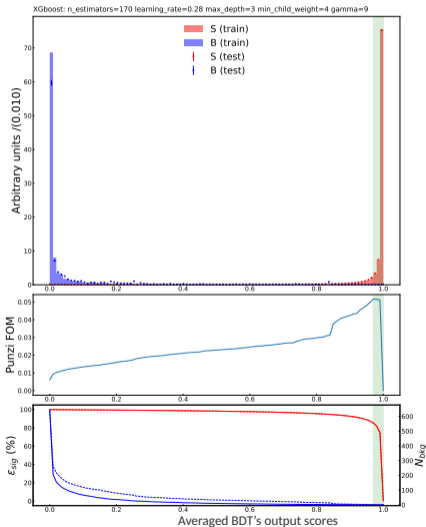
$\tau \rightarrow \mu \mu \mu$ - Background suppression: BDT (2)

Input BDT variable ranking according to :



| Event | Missing | Leptons | ROE | ROEmask | nROE | ROEThrust | CleoCones |
|--------------------------|--------------------|-------------------|------------------|-------------------------|---------------------------|-----------|---------------------|
| thrust | E_{miss}^{CMS} | $Li \theta^{CMS}$ | E_{ROE} | E_{ROE}^{mask} | nROEprong | thrustBm | cleoConeThrust_i |
| E_{vis}^{CMS} | $p_{miss}^{T,CMS}$ | | M_{ROE} | M_{ROE}^{mask} | nROEprong ^{mask} | thrustOm | cleoConeCollision_i |
| E_{γ}^{tot} | θ_{miss} | | P_{ROE} | P_{ROE}^{mask} | nROE γ | cosTBTO | |
| rank $p_{sig}^{T,CMS}$ | M_{miss}^2 | | P_{ROE}^T | $P_{ROE}^{T,mask}$ | nROE γ^{mask} | cosTBz | |
| rank E_{sig}^{CMS} | | | ΔE_{ROE} | ΔE_{ROE}^{mask} | nROEh ⁰ | | |
| χ^2_{vertex} | | | C_{ROE} | C_{ROE}^{mask} | nROEh ^{0,mask} | | |
| $cos(\theta_{p-vortex})$ | | | | | | | |
| nAllTracks | | | | | | | |
| nGoodTracks | | | | | | | |
| nPi0 | | | | | | | |
| nPhotonsFromPi0 | | | | | | | |

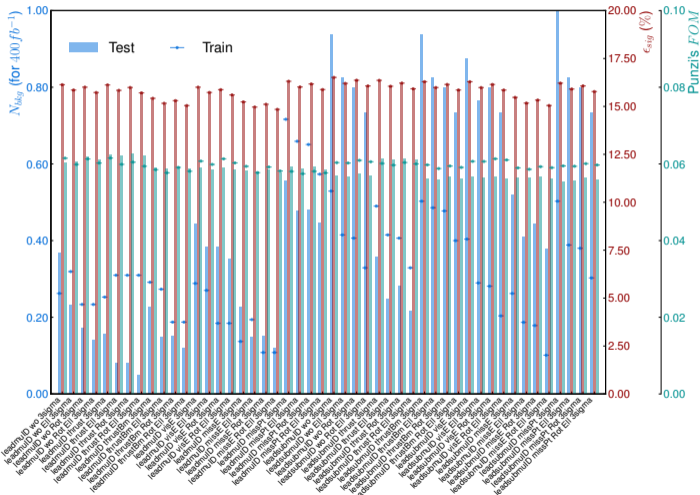
$\tau \rightarrow \mu \mu \mu$ - Background suppression: BDT (3)



BDT Results

- good separation between signal and background
- evolution of the log loss function are close for train and test samples
- define a cut on BDT output according to the Punzi FOM

$\tau \rightarrow \mu \mu \mu$ - Background suppression



Best configuration:

- $\mu ID_{lead} > 0.95$
- $0.89 < thrust < 0.97$
- $M'_{\mu\mu\mu}; \Delta E'_{\mu\mu\mu}$ signal region

with:

- $\epsilon_{sig} = 15.93\%$
- $N_{bkg} = 0.08$
- FOM = 0.062725

References in 3×1 topology:

- Belle 2 cut based analysis:
 $\epsilon_{sig} = 12.7\%$, $N_{bkg} = 0.2$
- Belle:
 $\epsilon_{sig} = 7.6\%$, $N_{bkg} = 0.13$
- Babar:
 $\epsilon_{sig} = 6.6\%$, $N_{bkg} = 0.44$

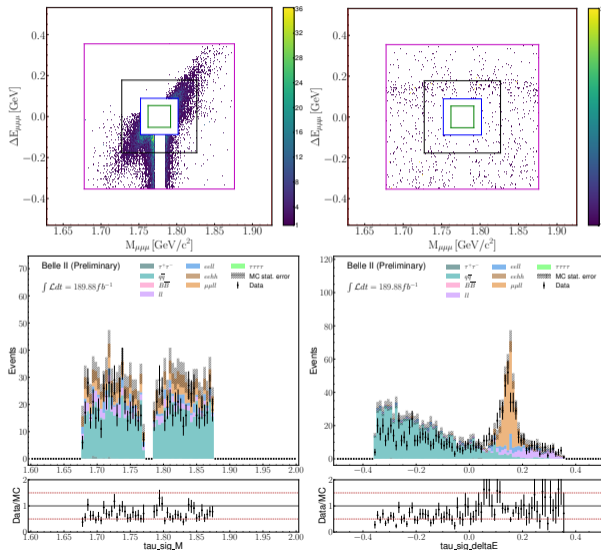
$\tau \rightarrow \mu \mu \mu$ - Data-MC comparison

Data/MC Comparison in sidebands

- Reconstruct $\tau \rightarrow \mu \mu \mu$ on 189.88 fb^{-1} data
- Blind:
 - inside sidebands the 5 to 20 Signal Region resolution
 - remove window $1.77 < M_\tau < 1.785$

Data/MC agreement

- Monte-Carlo Simulation (scaled):
1295.48 bkg evts
and **1.22% ϵ_{sig}**
- 189.88 fb^{-1} Data:**
910 evts



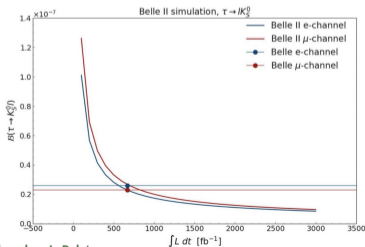
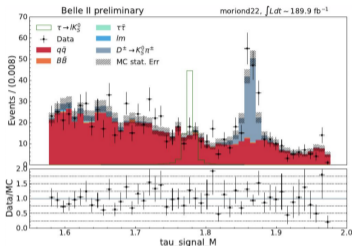


$\tau \rightarrow \ell K_S, \tau \rightarrow \ell \rho, \dots$

$\tau \rightarrow \ell K_S$

Klemens Lautenbach (CPPM)

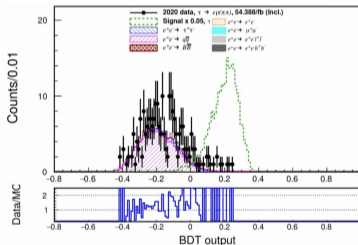
- Inclusive reconstruction.
- Overall good data-MC agreement outside of signal region.
- So far, no significant improvement expected w.r.t. Belle's upper limit (at 671 fb^{-1}).



$\tau \rightarrow \ell \rho$

Laura Zani (CPPM)

- Reconstruction similar to $\tau \rightarrow \ell \phi$.
- Data excess observed as well in electron channel.



Other ongoing studies:

- $\tau \rightarrow \ell + \alpha$ (invisible) (Cinvestav, HEPHY, DESY, MPP, Pisa)
- $\tau \rightarrow \ell \gamma$ (Cinvestav, DESY, Pisa).
- $\tau \rightarrow \Lambda \pi$ (Zhengzhou, Fudan).
- $\tau \rightarrow \ell K^*$ (CPPM) for the next GdR :)²



Summary

- Large variety of NP models predict lepton flavour violation, notably in tau decays.
- $\tau \rightarrow \mu \phi$ (leptoquark hypothesis for B -anomalies) and $\tau \rightarrow \mu \mu \mu$ (SUSY; background-free decay) are two of the “golden channels” studied at Belle II.
- $\tau \rightarrow \ell \phi$: analysis on $\sim 190 \text{ fb}^{-1}$ of data; muon channel at the level of Belle and competitive with BaBar for equivalent luminosities; room for improvement in both decay modes (missing background simulation, higher statistics in MC, hopefully better PID, ...).
- $\tau^- \rightarrow \mu^- \mu^+ \mu^-$: analysis on $\sim 190 \text{ fb}^{-1}$ of data; deploy BDT background rejection and inclusive reconstruction \rightarrow $2\times$ better efficiency than Belle, Babar studies and higher than Belle 2 cut based, see data deficit in data/MC comparison.
- Many other channels actively studied; in general, stay tuned for updates next year with full luminosity collected so far ($\sim 430 \text{ fb}^{-1}$)!

References I

-  Banerjee, S. et al. (2022). *Snowmass 2021 White Paper: Charged lepton flavor violation in the tau sector*. DOI: 10.48550/ARXIV.2203.14919. URL: <https://arxiv.org/abs/2203.14919>.
-  Calafiura, Paolo, David Rousseau, and Kazuhiro Terao (2022). *Artificial Intelligence for High Energy Physics*. WORLD SCIENTIFIC. DOI: 10.1142/12200. eprint: <https://www.worldscientific.com/doi/pdf/10.1142/12200>. URL: <https://www.worldscientific.com/doi/abs/10.1142/12200>.
-  Giffels, M. et al. (Mar. 2008). "The lepton-flavour violating decay $\tau \rightarrow \mu \mu \bar{\nu}_\mu$ at the LHC". In: DOI: 10.1103/PhysRevD.77.073010. URL: <http://arxiv.org/abs/0802.0049>.
-  Kou, E et al. (Dec. 2019). "The Belle II Physics Book". In: *Progress of Theoretical and Experimental Physics* 2019.12. ISSN: 2050-3911. DOI: 10.1093/ptep/ptz106. URL: <http://dx.doi.org/10.1093/ptep/ptz106>.

Backups

$\tau \rightarrow \ell \phi$ - Event reconstruction

Samples

Monte Carlo (MC) simulation:

- Signal: $\tau^\pm \rightarrow e^\pm \phi$; $\tau^\pm \rightarrow \mu^\pm \phi$
- Background: $\tau^+ \tau^-$, $q\bar{q}$, $B\bar{B}$, $\ell\ell(XX)$ ($\ell = e, \mu$; $X = e, \mu, \tau, \pi, K, p$).

Belle II data: 189.9 fb^{-1} (2019-2021).

Steps of the reconstruction

Track selections:

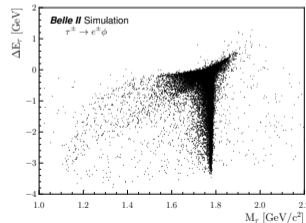
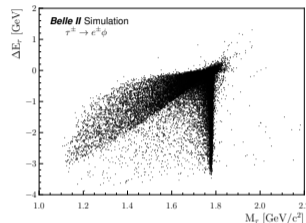
- Originate from the interaction point (IP): "good tracks"; at most 6 in event.
- Lepton tracks selected with particle identification variables (PID).
- Kaon tracks required to be in CDC acceptance \rightarrow no PID requirement but selection on ϕ mass instead: $1.014 < M_\phi < 1.024 \text{ GeV}/c^2$.

Final state radiations (FSR) = signal events displaced from signal region in $(M_\tau, \Delta E_\tau)$ space \rightarrow **Bremstrahlung corrections** on electron tracks to counteract efficiency loss.

Fit of τ and ϕ vertices.

Information on **Rest Of Event** (ROE, unused tracks and clusters) recovered for background suppression.

Events required to fire **low-multiplicity** Level1 (L1) ECL triggers.



$\tau \rightarrow \ell \phi$ - Background suppression: Variables

| Related to | Name | Definition |
|-------------------|--|---|
| Lepton | $E_{\text{lepton}}^{\text{CM}}$ | Energy in the center of mass frame (GeV). |
| | $p_{\text{lepton}}^{\text{T}}$ | Transverse momentum (GeV/c). |
| | $\theta_{\text{lepton}}^{\text{CM}}$ | Polar angle in the center of mass frame (rad). |
| Kaons | $\theta_{K_1 - K_2}$ | Angle between the two kaons (rad). |
| | KaonID of leading kaon | KaonID of the kaon with the highest transverse momentum. |
| 3-prong | $p_{\text{lead}}^{\text{T,CM}}, p_{\text{sub-lead}}^{\text{T,CM}}, p_{\text{third}}^{\text{T,CM}}$ | Transverse momentum in the center of mass frame of the leading, sub-leading and third 3-prong tracks (GeV/c). |
| ϕ meson | M_{ϕ} | Mass (GeV/c ²). |
| | E_{ϕ} | Energy (GeV). |
| | p_{ϕ}^{T} | Transverse momentum (GeV/c). |
| τ | — | τ thrust axis magnitude. |
| | $\cos \theta_{\tau-2}^{\text{thrust}}$ | Cosine of angle between τ thrust axis and z axis. |
| | $\theta_{\tau-\text{closest}}$ | Angle between τ and closest track (rad). |
| Vertexing | — | χ^2 probability of ϕ vertex fit result. |
| | — | χ^2 probability of τ vertex fit result. |
| Neutral particles | γ multiplicity | Number of photons in event. |
| | π^0 multiplicity | Number of neutral pions in event. |
| | γ from π^0 multiplicity | Number of photons produced by π^0 decays in event. |

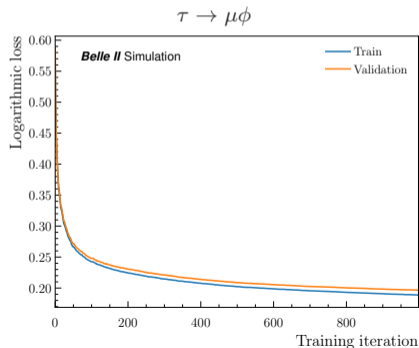
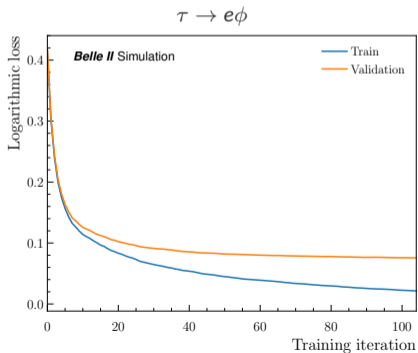
| Related to | Name | Definition |
|---------------------|---|---|
| Missing momentum | M_{miss}^2 | Missing mass squared (GeV ² /c ⁴). |
| | $E_{\text{miss}}^{\text{CM}}$ | Energy in the center of mass frame (GeV). |
| | $p_{\text{miss}}^{\text{T}}$ | Transverse momentum (GeV/c). |
| | θ_{miss} | Polar angle (rad). |
| | $\cos \theta_{\text{lepton-miss}}$ | Cosine of angle between lepton and missing momentum. |
| Event | — | Number of tracks. |
| | — | Number of good tracks. |
| | — | Thrust axis magnitude. |
| | $E_{\text{vis}}^{\text{CM}}$ | Visible energy in the center of mass frame (GeV). |
| | R_2 | Reduced Fox-Wolfram moment $R_2 = H_2/H_0$. |
| CLEO thrust 0, 1, 2 | — | 0 th , 1 st , 2 nd order CLEO cone with respect to thrust axis (GeV/c). |
| | — | 0 th , 1 st , 2 nd order CLEO cone with respect to collision axis (GeV/c). |
| Rest Of Event | — | ROE thrust axis magnitude. |
| | $\cos \theta_{\tau-\text{ROE}}^{\text{thrust}}$ | Cosine of angle between τ and ROE thrust axes. |
| | $M_{\text{ROE(masked)}}$ | Mass of the masked ROE (GeV/c ²). |
| | $E_{\text{ROE(masked)}}$ | Energy of the masked ROE (GeV). |
| | $\Delta E_{\text{ROE(masked)}}$ | Difference between the energy of the masked ROE and half the center of mass energy (GeV). |
| | $p_{\text{ROE(masked)}}$ | Momentum of the masked ROE (GeV/c). |
| | $p_{\text{ROE(masked)}}^{\text{T}}$ | Transverse momentum of the masked ROE (GeV/c). |
| — | Total charge of masked ROE. | |
| — | Number of charged particles in masked ROE. | |
| — | Number of photons in masked ROE. | |
| — | Number of neutral hadrons in masked ROE. | |



$\tau \rightarrow \ell \phi$ - Background suppression: BDT optimisation

Mitigation of overfitting

- Early stopping implemented: logloss in training sample vs validation sample.
- BDT parameters tested (max. tree depth, min. loss reduction, ...), selected according to area under receiver operating characteristic (ROC) curve in validation sample.



$\tau^- \rightarrow \mu^- \mu^+ \mu^-$ - BDT overtraining health

Train & Validation Logloss in function of the boosting rounds to visualize the training behaviour:

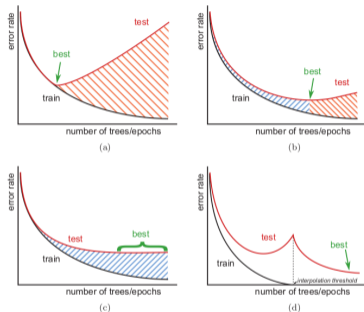
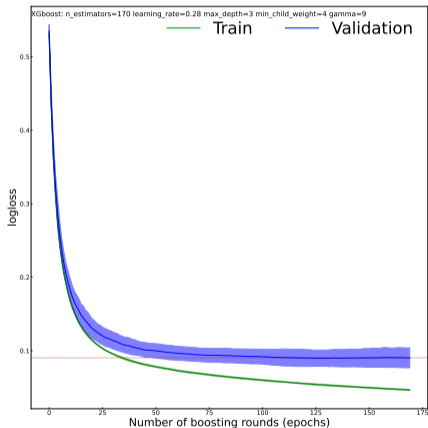


Fig. 3. Overtraining estimation using the error rate as a function of the number of trees (for boosted decision trees) or epochs (for neural networks). Black curves are measured on the training sample and red curves on the validation sample. The optimal classifier corresponds to the "best" label. The hatched areas represent overtraining: beneficial in blue (but underfitting), detrimental in orange (overfitting). (a) Typical curves, with the best model at the minimum of the testing curve, and overfitting beyond with decrease of performance. (b) The best model is overtrained but still improves performance. (c) Typical curves for boosted decision trees with flattening testing error rate: all models in the flat area perform equally well despite increasing overtraining. (d) Interpolation regime: the best classifier is obtained after the training error has reached zero.

P. Calafiura et al., Artificial Intelligence for High Energy Physics